



HAL
open science

Quantifying glass powder reaction in blended-cement pastes with the Rietveld-PONKCS method

Mehdi Mejdi, William Wilson, Mickael Saillio, Thierry Chaussadent, Loïc Divet, Arezki Tagnit-Hamou

► **To cite this version:**

Mehdi Mejdi, William Wilson, Mickael Saillio, Thierry Chaussadent, Loïc Divet, et al.. Quantifying glass powder reaction in blended-cement pastes with the Rietveld-PONKCS method. *Cement and Concrete Research*, 2020, 130, 27 p. 10.1016/j.cemconres.2020.105999 . hal-02651106

HAL Id: hal-02651106

<https://hal.science/hal-02651106v1>

Submitted on 29 May 2020

HAL is a multi-disciplinary open access archive for the deposit and dissemination of scientific research documents, whether they are published or not. The documents may come from teaching and research institutions in France or abroad, or from public or private research centers.

L'archive ouverte pluridisciplinaire **HAL**, est destinée au dépôt et à la diffusion de documents scientifiques de niveau recherche, publiés ou non, émanant des établissements d'enseignement et de recherche français ou étrangers, des laboratoires publics ou privés.

1 Quantifying glass powder reaction in blended-cement 2 pastes with the Rietveld-PONKCS method

3 Mehdi Mejdi^{a,b}, William Wilson^b, Mickael Saillio^a, Thierry Chaussadent^a, Loic Divet^a, and
4 Arezki Tagnit-Hamou^b

5
6 ^a Université de Paris-Est, MAST, CPDM, IFSTTAR F-77447 Marne-La-Vallée, France

7 ^b Département de Génie Civil, Université de Sherbrooke, Sherbrooke (Québec), J1K 2R1,
8 Canada

9 10 **Abstract**

11 X-ray diffraction (XRD) is a prominent technique to characterise cement-based materials. The
12 combination of the Rietveld refinement with the Partial Or No Known Crystal Structure
13 (PONKCS) approach now enables the quantification of both crystalline phases and
14 amorphous contribution of SCMs. This paper describes the application of Rietveld-PONKCS
15 to determine the amount of reacted glass powder (GP) in blended cement pastes. The accuracy
16 and precision of the method were compared to the results of independent methods such as
17 selective acid dissolution, thermogravimetric analysis (TGA) combined to energy-dispersive
18 spectroscopy (EDS) or inductively coupled plasma (ICP) applied to GP-lime mixtures. For
19 blended cement, the consistency of the method was internally checked using the standard
20 addition method. Overall, an average precision of 1.6 wt.% and accuracy better than 1.5 wt.%
21 were found for Rietveld-PONKCS applied to GP containing systems.

22 **Keywords**

23 X-ray diffraction, PONKCS, amorphous supplementary cementitious materials, soda-lime
24 glass powder, blended cement

25 26 **1. Introduction**

27 Contributing to the efficient use of natural resources, the cement industry provides an added-
28 value recovery option for various wastes and industrial by-products (e.g. thermal power plant
29 fly ashes or post-consumption glass powder). These supplementary cementitious materials

30 (SCMs) are usually high-potential reactive materials used as an addition or in substitution to
31 cement [1]. Their reaction mechanisms occur in synergy with the cement hydration and
32 induce changes in the amounts and the types of the formed hydrates, the porous network, and
33 therefore the durability of the concrete [1–5]. However, the use of novel pozzolanic SCMs is
34 rather restricted to low substitution rates due to the challenges in understanding their
35 reactivity in blended cementitious systems [1,6]. Therefore, further increase in SCMs dosages
36 is closely linked to the development of techniques that accurately quantify their reactivity and
37 their impact on the phase assemblage in the cementitious matrix [6]. In this context, different
38 methods have been employed to assess the extent of SCMs' reaction. Nevertheless, most
39 methods are subject to limitations and cannot be relevant for all SCMs currently available and
40 under development. Direct and indirect methods for the determination of the SCMs hydration
41 degree have been reviewed by several authors (e.g. RILEM TC 238-SCM committee) [7–9]:

- 42 • The selective dissolution approach has been by far the most reported in the literature
43 over the past decades [10–15]. This method consists fundamentally of a preferential
44 acid dissolution of the cement and hydrates while keeping the unreacted SCM
45 particles intact. However, the application of this method has been associated with
46 important uncertainties and showed considerable discrepancies with other methods
47 [6,8,14,16]. These non-quantifiable errors are mainly related to the incomplete
48 dissolution of the clinker and its hydrates and/or the partial dissolution of the SCMs
49 [7,14,16].
- 50 • Backscattered electron image analysis (SEM-IA) is restricted by the resolution limit of
51 the SEM to particles with a size greater than $\sim 2 \mu\text{m}$. Therefore, in addition to being
52 time-consuming, this approach is irrelevant to fine materials such as silica fume or
53 metakaolin [6,9,16].
- 54 • Different portlandite consumption approaches have been developed as indirect
55 methods to estimate the pozzolanic reaction of SCMs in cement pastes. The
56 stoichiometric amount of SCM required to react can be retrieved using the portlandite
57 consumed (measured by thermogravimetric analysis) and the Ca/Si ratio of the C-S-H
58 (often measured by EDS). However, this approach is sensitive to even relatively small
59 errors in the measurement of portlandite content or Ca/Si ratio, and might lead to large
60 uncertainties [8].

- 61 • Nuclear magnetic resonance (^{27}Al and ^{29}Si) spectroscopy is one of the direct methods
62 that can be used with good accuracy. However, in addition to being time demanding,
63 the NMR equipment is not readily available [17].
- 64 • Additionally, other indirect methods (such as calorimetry, chemical shrinkage, and
65 bound water) are also commonly used to assess the reacted amounts of SCMs.
66 Nonetheless, the translation of the results of these methods in terms of degree of
67 hydration is still an outstanding issue [18,19].

68

69 The analysis of X-ray diffraction (XRD) patterns is another prominent technique in the
70 characterisation of crystalline phases. Due to the ease and speed of the measurement, this
71 technique has been applied to cement based materials [20–25]. Moreover, given the
72 robustness of today’s computation tools, the full-pattern Rietveld [26] quantification method
73 can reliably deal with complex diffraction patterns with strong overlapping peaks. However,
74 the Rietveld method can only be applied to crystalline phases with known structures.
75 Therefore, other techniques are commonly combined with Rietveld refinement in order to
76 determine the amount of amorphous/unidentified phases, such as the internal standard method
77 or the external standard method (G-factor method) [27–29]. These approaches can determine
78 the total content of amorphous phases but fail to distinguish the contributions of each
79 amorphous material. For this purpose, Scarlett and Madson [30] have developed a direct
80 approach for quantitatively analysing phases with “Partial Or No Known Crystal Structure”
81 (PONKCS). This approach can be used for the quantification of amorphous phases, which are
82 then defined as a “set of related peaks”. Recently, the PONKCS method has been successfully
83 adopted to measure the reaction’s degree of supplementary cementitious materials in blended
84 cement, since they are predominately amorphous [6–8,31–33].

85 Though the use of this method for conventional SCMs has been previously assessed [6–
86 9,33,34], further work is required for the application the Rietveld-PONKCS approach to
87 quantify the degree of reaction of alternative cementitious materials, such as Glass Powder
88 (GP). GP is obtained by micronizing post-consumption soda-lime glass bottles and its use in
89 concrete offers a viable opportunity to answer the current demand of highly sustainable
90 concrete [5,35,36]. The predominant amorphous phase, mainly composed of silica, provides
91 the required components to exhibit high pozzolanic properties. Therefore, an optimal
92 industrial use of GP depends on improving the understanding of its reaction in blended-
93 cement systems. In this respect, the present study explores the reliability and precision of
94 Rietveld-PONKCS method for the quantification of glass powder (GP) degree of reaction in

95 binary systems. Moreover, the results of this XRD-based technique are compared to other
 96 independent methods such as selective acid dissolution and portlandite consumption. The
 97 consistency of the PONKCS measurements is verified first on synthetic systems consisting of
 98 portlandite and glass powder pastes, and then on cement pastes in order to test the relevance
 99 of this technique compared to the widespread methods.

100 2. Materials and methods

101 2.1 Materials and sample preparation

102 The study focuses on the measurement of the degree of reaction of post-consumption soda-
 103 lime glass powder, as a supplementary cementitious material (SCM). The hydration of GP
 104 was investigated within Portlandite pastes ($\text{Ca}(\text{OH})_2$, also known as CH) and commercially
 105 available Ordinary Portland Cement (OPC) pastes. **Table 1** presents chemical and mineral
 106 compositions of the raw materials, as obtained by X-ray Fluorescence and X-ray Diffraction
 107 with Rietveld quantification. **Table 2** shows the physical properties obtained by laser
 108 granulometry, pycnometry, Blaine, and nitrogen adsorption tests. The Mass Absorption
 109 Coefficients (MAC, also μ) were calculated from chemical compositions and the international
 110 tables of crystallography for $\text{CuK}\alpha$ radiation [37], with the Loss of Ignition (LOI) attributed to
 111 water.

112 **Table 1. Chemical and mineral compositions of used materials**

	SiO ₂	CaO	Al ₂ O ₃	Fe ₂ O ₃	Na ₂ O	K ₂ O	P ₂ O ₅	SO ₃	MgO	TiO ₂	LOI*	MAC
CH	--	73.98			—			0.07	0.11		25.79	93.55
GP	71.11	10.04	1.81	0.36	13.06	0.56	0.02	0.14	1.21	0.06	1.79	44.89
OPC	19.52	60.57	4.41	2.63	0.31	0.90	0.89	4.01	2.84	0.21	2.74	93.91

113 * Loss on ignition at 1000°C

114

	C ₃ S	C ₂ S	C ₃ A	C ₄ AF	CH	Calcite	Quartz	Gypsum	Bassanite	Periclase	Amorphous*
CH					95.1	0.8	—				4.1
GP					—	0.5	0.7				98.9
OPC	52.1	11.5	4.3	8.6	—	3.3	0.3	3.4	2.6	0.6	12.8

115 * Amorphous or/and unidentified obtained using external standard

116

117 **Table 2. Physical properties of used materials measured by laser granulometry, pycnometry, Blaine and**
 118 **BET tests.**

	D ₅₀ (μm)	Density	Blaine (m ² /kg)	BET (m ² /g)
CH	5.3	2.23	—	—

GP	10.2	2.54	593	0.70
OPC	16.3	3.11	395	1.26

119

120 Pastes of glass powder and $\text{Ca}(\text{OH})_2$ were prepared with a propeller mixer (2 min, 2000 rpm)
 121 under nitrogen atmosphere, with GP:CH mass ratios of 1:3, 1:1, and 3:1. The water-to-binder
 122 (w/b) mass ratio was fixed to 0.75 to obtain a sufficient workability. The samples were cast
 123 into sealed containers and preserved in a desiccator until testing ages of 7, 14, 28, 56, and 91
 124 days. Before each test, the samples were ground to an average diameter of $d_{50}=40 \mu\text{m}$, and the
 125 hydration was stopped using two solvent exchanges (isopropanol and diethyl ether). The
 126 solvents were removed first by filtration and then by vacuum drying. On the other hand, three
 127 sets of cement pastes were prepared with partial substitution (wt.%) of Portland cement
 128 (OPC) by glass powder at different rates: the system OPC with 100% Portland cement, the
 129 system 10GP with 10% of glass powder (90% OPC) and the system 20GP (80% OPC+20%
 130 GP), as reported in **Table 3**. The cement pastes were prepared with a w/b mass ratio of 0.485
 131 using a high-shear mixer. The same conservation and hydration stoppage procedures, used for
 132 CH mixtures, were applied to GP-OPC systems.

133

Table 3. Mix design for CH and OPC pastes

Ca(OH)₂ mixes	GP:CH ratio	W/B	Cement pastes	GP:OPC ratio	W/B
25GP	25:75	0.75	OPC	0:100	0.485
50GP	50:50	0.75	10GP	10:90	0.485
75GP	75:25	0.75	20GP	20:80	0.485

134

135 2.2 Thermogravimetry

136 Thermogravimetric analyses (TGA) were conducted using a TA instrument SDT Q600. The
 137 analysis was run with ~50 mg samples over a temperature range of 30–1000°C with a heating
 138 rate of 20°C/min. N_2 was used as a purging gas at a rate of 50mL/min. TGA investigations
 139 allowed the determination of bound water and the mass loss corresponding to the portlandite
 140 decomposition. The bound water content was used to normalise the initial content of reactants
 141 and calculate the MAC of hydrated samples, which was necessary for the quantification of
 142 XRD patterns using the external standard method.

143 2.3 Selective acid dissolution and ICP-AES

144 Selective dissolution was used to determine the amount of unreacted GP in hydrated samples.
145 The method was first carried out on anhydrous (raw) materials to test the effectiveness of the
146 technique and to measure their dissolution. The values of the insoluble residues (97.9% for
147 GP and 0.1% for CH) were used later to correct the unreacted GP measured in hydrated
148 mixes. The dissolution was performed as follows: 1g (± 0.0005 g) of sample after hydration
149 stoppage was placed in a beaker with 3 ml of HNO₃ and 97 ml of distilled water. The acid
150 attack was continued for 30 min under continuous stirring. In order to determine the residue,
151 the solution was first filtered using a 0.7-1 μ m ashless filter paper, the residue with the filter
152 was placed in a crucible, put in a furnace at 1000°C and then weighed.

153 On the other hand, the filtrate (100 ml) was diluted with distilled water to reach 1 L and
154 analysed using Inductively Coupled Plasma Atomic Emission Spectroscopy (ICP-AES). The
155 concentrations of silicon, sodium and calcium elements were quantified using an ULTIMA
156 2000 ICP-AES (Jobin Yvon Horiba).

157 **2.4 X-ray diffraction data collection**

158 A PANalytical X'pert Pro MRD diffractometer was used to acquire the X-ray powder
159 diffraction patterns at 50 mA and 40 kV. Measurements were performed on flat surfaces of
160 back-loaded samples with a Bragg-Brentano (θ - 2θ) geometry, using Soller slits of 0.04 rad,
161 incident divergence and anti-scatter slits of 0.5°. A PIXcel 1D detector with an active length
162 of 3.347 ° 2θ was used for the data collection. The acquisition was performed over an angular
163 range of 5 to 70° 2θ with a step size of 0.0263° 2θ and a counting time of 176 s (i.e. 720
164 ms/step), resulting in a time of 30 min per scan. During the scans, the samples were spun at 8
165 rpm around the vertical goniometer axis to improve particle statistics. A corundum powder (α -
166 Al₂O₃) was used as an internal and external standard (Alfa Aesar, crystallinity calibrated to
167 98.2% using the NIST SRM676a standard). The standard was frequently tested to consider the
168 attenuation of the X-ray tube intensity.

169 **2.5 Quantitative XRD analysis**

170 The XRD experimental patterns were modelled using Xpert HighScore Plus 4.7a from
171 PANalytical. The approach used for the profile fitting can be divided into three key steps, as
172 proposed by Stetsko et al. [32]:

173 ***a) Traditional Rietveld with only the crystalline phases***

174 In this step, a high order Chebyshev polynomial background (a 6th order in this study) is
175 required to exclude all the amorphous content from the calculation. During the refinement,

176 some parameters were subject to restrictions to avoid an unrealistic fit with aberrant values for
 177 the crystal parameters. Therefore, the lattice parameters variation was limited to a range of
 178 1% and the Full Width at Half-Maximum (FWHM) to a range of 0.0001–0.2. The peak shape
 179 and the preferential orientation parameters were adjusted iteratively on raw materials only
 180 when necessary (i.e. in the case of a high weighted profile residue or a high goodness of fit)
 181 and then kept constant for the rest of the analysis. Following the refinement, the scale factors
 182 and cell volumes were used to estimate the absolute weight fraction of each phase using the
 183 external standard method (Eq. 1). The mass attenuation coefficient (MAC, μ) for each sample
 184 was derived from XRF chemical composition for anhydrous samples, and by a combination of
 185 XRF and TGA for hydrated samples.

186

$$w_{\alpha} = \frac{S_{\alpha} \cdot (ZMV)_{\alpha}}{S_{ES} \cdot (ZMV)_{ES}} \frac{\mu_{sample}}{\mu_{ES}} w_{ES,crist} \quad (1)$$

$$w_{amorphous} = 1 - \sum_{\alpha}^{np} w_{\alpha} \quad (2)$$

187 Where:

- w_{α} : Weight fraction of phase α
- $w_{amorphous}$: Weight fraction of the total amorphous content
- $S_{\alpha,ES}$: Refined scale factor of phase α , or of external standard (ES)
- Z, M, V : Number of formula units per unit cell, the mass of the formula unit and the unit cell volume
- $\mu_{sample,ES}$: Mass absorption coefficient of phase α (or ES)
- $w_{ES,crist}$: Crystallinity of the external standard
- np : Number of phases included in the calculation

188

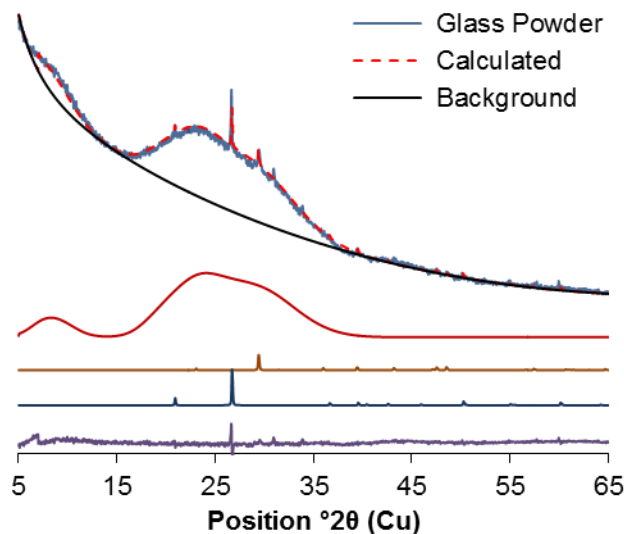
189 ***b) Definition and calibration of the PONKCS pseudo-structure***

190 The use of a PONKCS phase allows the quantification of a specific amorphous material (e.g.
 191 SCMs), by fitting a pseudo-structure to the amorphous contribution of the material to the

192 XRD pattern (see Fig 1). The pseudo-phase can be defined using an existing “hkl phase” with
193 partial structure information or a newly defined set of related peaks with no structure
194 information [30]. It is also worth mentioning that the amorphous hump can be fitted easily
195 with a variety of space groups. Another parameter affecting the accuracy of the PONKCS
196 phase quantification is the choice of the background. Different choices of the background
197 have been reported in the literature. Madsen et al. [38] used a third order Chebyshev
198 polynomial with a $1/2\theta$ parameter, while Snelling et al. [6] reported that a first order
199 Chebyshev polynomial with a $1/2\theta$ parameter gives the best fit. On the other hand, Stetsko et
200 al. [32] recommended the use of a first-order polynomial background. Otherwise, the
201 background can also be fitted manually, but this will alter the inter-laboratory reproducibility
202 of the method since it depends mainly on the user's judgement.

203 In this study, the glass powder was defined as a single phase using a set of pseudo-Voigt
204 peaks while the C-S-H was modelled using an “hkl file” based on Tobermorite 14 \AA crystal
205 structure [39]. The diffuse scattering signals of amorphous phases were then refined using the
206 Pawley curve fitting algorithm on a 100% anhydrous GP sample for glass powder (see Fig. 1)
207 and a 180 days hydrated sample of silica fume and portlandite (ratio of 1 to 3) for C-S-H. In
208 this study, a first-degree polynomial background with a $1/2\theta$ parameter produced the most
209 reliable fit when using the PONKCS phases. Therefore, this type of background was adopted
210 for all analyses, i.e., for both raw materials and hydrated samples.

211



212

213

Fig. 1. Decomposition of a pure glass powder XRD pattern

214

215 After the definition of the PONKCS phase, the quantification required the calibration of the
216 pseudo-phase. Therefore, the “ZMV constant” was determined by the internal standard
217 method (Eq. 3) using a 50:50 reference mix of the glass powder and the highly crystalline
218 corundum. It is worth mentioning that the ZM and V values have no physical meaning; they
219 represent an empirical definition of the pseudo-phase for use in the Rietveld refinement.

$$\frac{W_{\alpha}}{W_{\text{strd}}} = \frac{S_{\alpha}(\text{ZMV})_{\alpha}}{S_{\text{strd}}(\text{ZMV})_{\text{strd}}} \quad (3)$$

220 On the other hand, the C-S-H weight percent in the hydrated samples was determined by
221 difference using the external standard method (instead of a calibration constant for the C-S-H
222 PONKCS phase). This approach was preferred to account for the expected variation of C-S-H
223 composition over the hydration time.

224 *c) Insertion of the calibrated PONKCS phase in the refinement*

225 With the ZMV constant, all the parameters needed to quantify the PONKCS phase are
226 available. The new phase can then be implemented in the Rietveld refinement of an unknown
227 sample, and its weight percentage is calculated based on the defined ZMV constant and its
228 refined scale factor. During the refinement with the PONKCS phase, the refined parameters
229 obtained for the crystalline phases in “step a” were kept constant, while only the background
230 was changed to a polynomial with a $1/2\theta$ parameter and the PONKCS phase was included in
231 the refinement. In the second iteration, all the scale factors were refined simultaneously.

232 **2.6 SEM-EDS (QEDS)**

233 The scanning electron microscopy was carried out with a Hitachi S-3400 N SEM equipped
234 with an Oxford Inca Energy 250 energy-dispersive spectrometer (EDS). The hydration was
235 stopped by solvent exchange in isopropanol, which allowed the removal of free water. The
236 samples were coarsely ground and mixed in a fast-setting epoxy resin. Once the resin has
237 hardened, the specimens were planarized using a 600 grit SiC paper then polished using a
238 perforated cloth with 3 μm and 1 μm diamond suspensions with isopropanol as a lubricant.
239 Before the analysis, the samples were degassed under vacuum for 2h and coated with about
240 15 nm of carbon to avoid surface charging during SEM analysis. The observations were
241 performed with a magnification of 400 \times and an accelerating voltage of 15 kV, allowing the
242 analysis over a region of interest of 300 μm \times 240 μm .

243 The chemistry of around 700 micro-volume was investigated using an energy-dispersive X-
244 ray spectroscopy (EDS) point analysis. A counting time of 20 s per spot was employed to

245 obtain quantifiable and high quality spectra. Afterwards, the quantitative analyses (QEDS)
 246 were achieved by post-processing the EDS spectra with the NIST software DTSA-II and
 247 using synthetic standards to calibrate the quantification (pure C₂S for *Ca* and *Si*, pure C₃A for
 248 *Al*, olivine for *Mg* and *Fe*, anhydrite for *S*, orthoclase for *K*, tugtupite for *Na* and *Cl*, and
 249 sphene for *Ti*). Finally, invalid measurements due to micro-cracked products and local
 250 charging were eliminated based on the Duane-Hunt limit.

251 3. Results

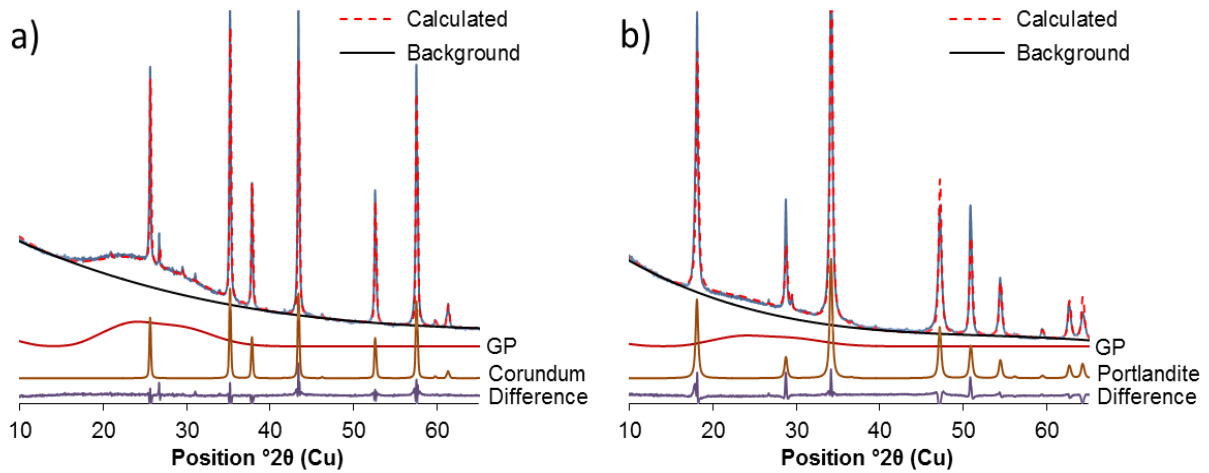
252 3.1 Calibration of the PONKCS method for GP

253 The repeatability (95% confidence interval) and the accuracy (i.e. bias between the PONKCS
 254 measures and the true weighed values) of the developed quantification method were first
 255 evaluated on simple anhydrous binary systems. Homogenised mixes of varying proportions of
 256 GP and corundum/portlandite were prepared to calibrate the pseudo-phase (see [table 4](#)).
 257 Triplicate measurements were done on arbitrary samples, prepared separately with the same
 258 composition, to assess the error related to the sample preparation (i.e. repeatability of the
 259 measurement). The decomposition of the calculated patterns, showing the contribution of each
 260 phase, is illustrated in [Fig 2](#).

261 **Table 4. Composition of the anhydrous systems employed to assess the accuracy and precision of the**
 262 **PONKCS method applied to GP.**

Dry samples	GP	CH	Corundum
10GP90Corr (x3)	10		90
20GP80Corr (x3)	20		80
30GP70Corr	30		70
50GP50Corr (x3)	50		50
70GP30Corr	70		30
90GP10Corr (x2)	90		10
25GP75CH	25	75	
50GP50CH (x3)	50	50	
75GP25CH	75	25	

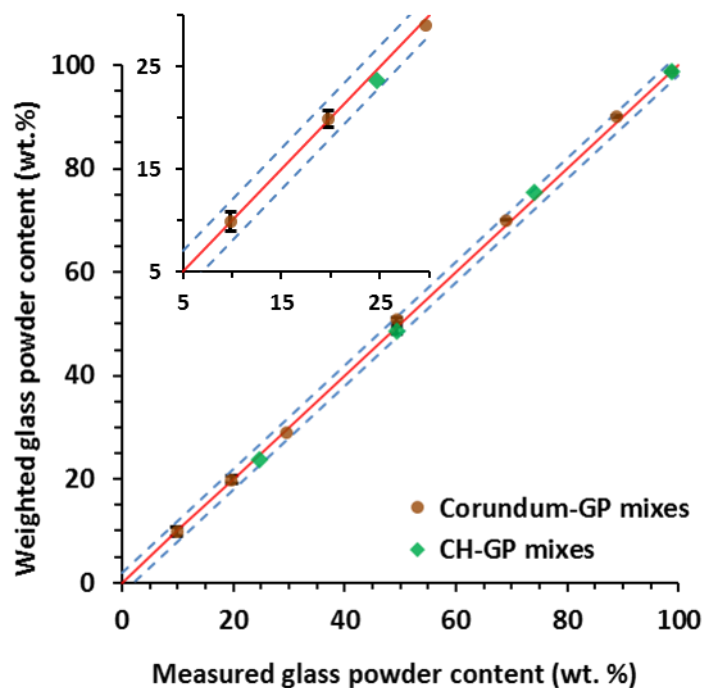
263



264

265 **Fig. 2. XRD pattern decomposition of preblended anhydrous samples: a) 50GP50Corr and b) 25GP75CH.**
 266 **The experimental and calculated patterns are shown respectively in blue and dashed-red lines.**

267 For the mixes performed in triplicate, the results showed a 2σ repeatability of 0.65% on
 268 average, without exceeding 0.93%. Moreover, the average measured-weighed bias was 0.9
 269 wt.% (max 1.5 wt.%). Considering that the sample homogenisation may be more limiting than
 270 the XRD analysis procedure itself [6], it can be concluded that the method shows a high
 271 precision and a high accuracy in the quantification of GP in anhydrous mixes (within 1.5% of
 272 the weighed amount of SCM). The correlation between the measured and weighed amounts of
 273 GP is shown in Fig 3.



274

275 **Fig. 3. Correlation between the weighed and measured glass powder content (wt. %) in the simulated**
 276 **anhydrous mixes with corundum and portlandite. The red line shows the 1:1 correlation while the dashed**
 277 **blue lines represent a tolerance interval of +/- 2 wt. %. The error bars describe the repeatability of the**
 278 **measurement.**

279 **3.2 Assessment of the PONKCS reliability in hydrated systems with GP**

280 The hydration of cement leads to the formation of amorphous products, mainly C-S-H. This
281 adds a level of complexity to quantitative analysis of the degree of reaction of SCMs due to
282 the potential overlap between the SCMs and C-S-H amorphous humps. To address this issue,
283 the Rietveld-PONKCS method was tested for different blended systems of increasing
284 complexity: first, for hydrated mixes of GP and portlandite simulating the pozzolanic reaction
285 (with 25, 50 and 75% GP), and then for blended cement pastes with 10% and 20% GP
286 replacements to analyse the reactivity of the glass powder in cementitious matrices. As an
287 example, Fig. 4 depicts the deconvolution of XRD patterns of hydrated GP-CH systems after
288 28 days of hydration. An increase of residual amorphous GP in increasing initial GP content
289 is clearly shown in Fig. 4 and the results are further discussed in the next subsections, along
290 with results of other independent methods used to cross-check the Rietveld-PONKCS
291 analyses.

292

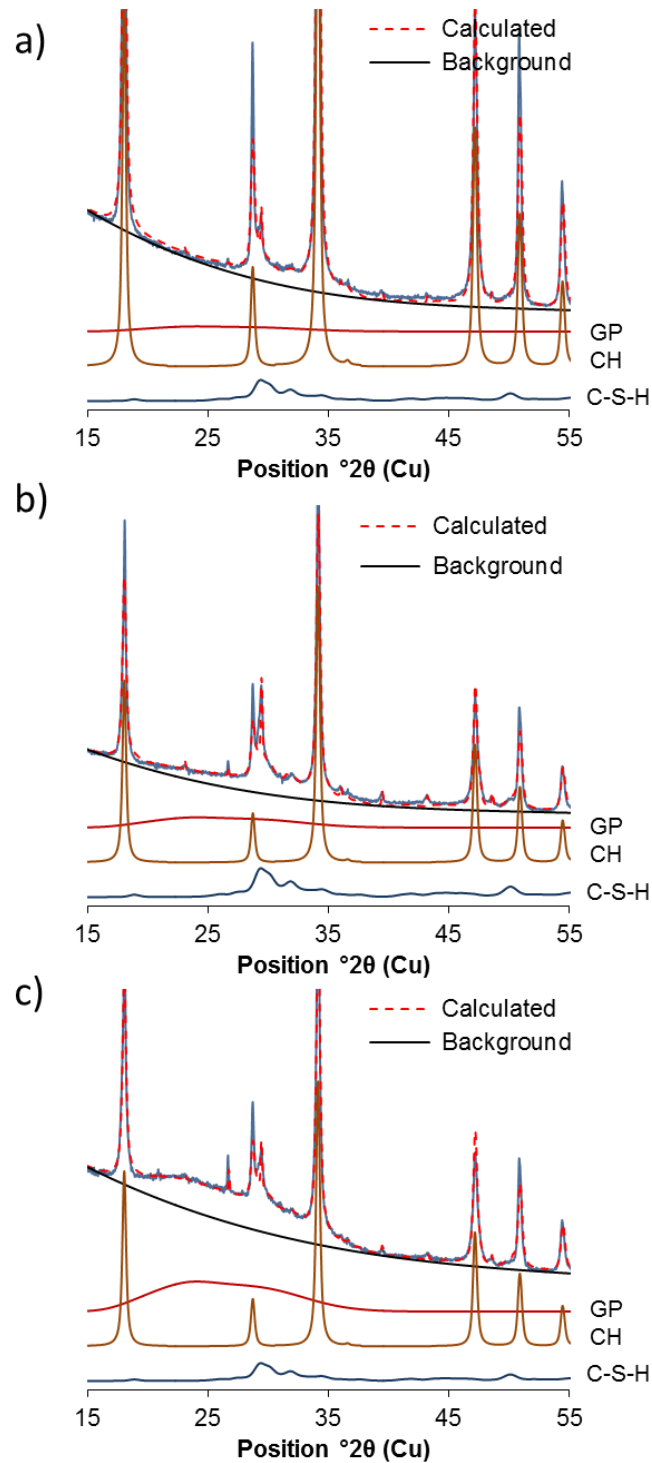


Fig. 4. XRD pattern decomposition of 28-day hydrated GP-CH systems: a) 25GP and b) 50GP and c) 75GP.

293

294
295

296 3.2.1 Comparison of independent methods for the quantification of GP in synthetic systems

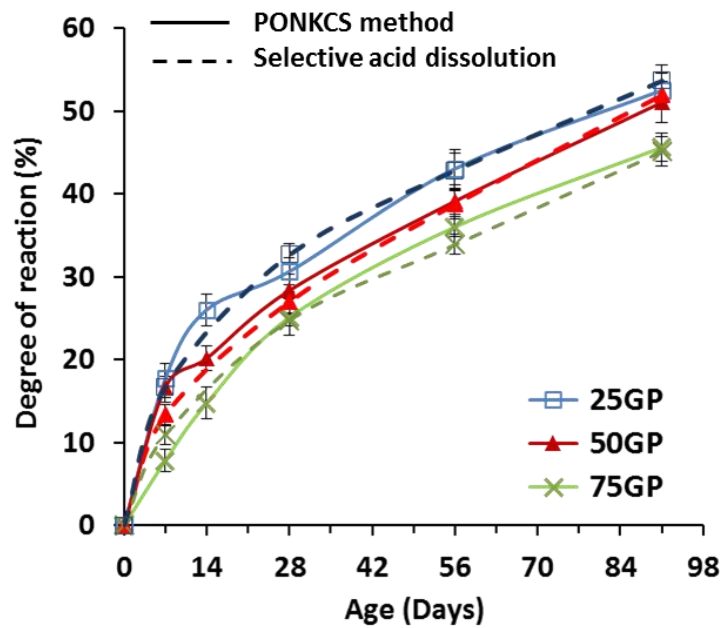
297 a) Direct methods for the quantification of unreacted GP

298 The Rietveld-PONKCS method was first applied to simple hydrated mixes of GP and
 299 portlandite, and the extent of reaction of GP was determined at 7, 14, 28, 56, and 91 days. The
 300 degree of reaction of GP, normalised to the initial amount in the mix (i.e., corrected with the

301 bound water), was compared in Fig 5 with the results of the insoluble residue after acid
302 dissolution. Overall, the two methods show very comparable results, with an average
303 difference of the unreacted GP content of 0.7 wt.% (max 2.1 wt.%).

304 It is worth mentioning that due to the variation of GP content in the mixes, a variation in the
305 hydrate composition is also expected. However, the aim of this paper is the quantification of
306 the degree of reaction of GP, whereas the hydration products are further discussed in [40].

307



308

309 **Fig. 5. Comparison of the degree of reaction of GP measured by Rietveld-PONKCS and by acid**
310 **dissolution methods. The error bars show ranges of measurements.**

311

312 ***b) Indirect methods and mass balance analyses***

313 The amount of reacted SCMs can also be obtained indirectly based on the consumed
314 portlandite (often measured by TGA) and the composition of the formed hydrates. The degree
315 of reaction of SCMs is then calculated based on the amount of silica required to react with
316 portlandite to reach the measured Ca/Si of the C-S-H. This method assumes that the totality of
317 the dissolved silica from the SCM reacts with portlandite to form C-S-H. In the case of simple
318 CH-GP systems, this assumption is realistic and therefore the degree of reaction (i.e. the
319 reacted amount) of GP can be retrieved using equation 4.

$$\alpha_{GP} = \frac{W_{CH\ consumed,TGA} \frac{W_{CaO,CH}}{M_{CaO}}}{\left(Ca/Si_{CSH} - \frac{W_{CaO,GP}}{W_{SiO_2,GP}} \frac{M_{SiO_2}}{M_{CaO}} \right) \cdot f \cdot \frac{W_{SiO_2,GP}}{M_{SiO_2}}} \quad (4)$$

320 With:

α_{GP} : Degree of hydration

$W_{CH\ consumed,TGA}$: Weight of consumed CH

$W_{oxide,material}$: Weight percentage of oxide (CaO, SiO₂) in material (CH, GP)

M_{oxide} : Molar mass of oxide

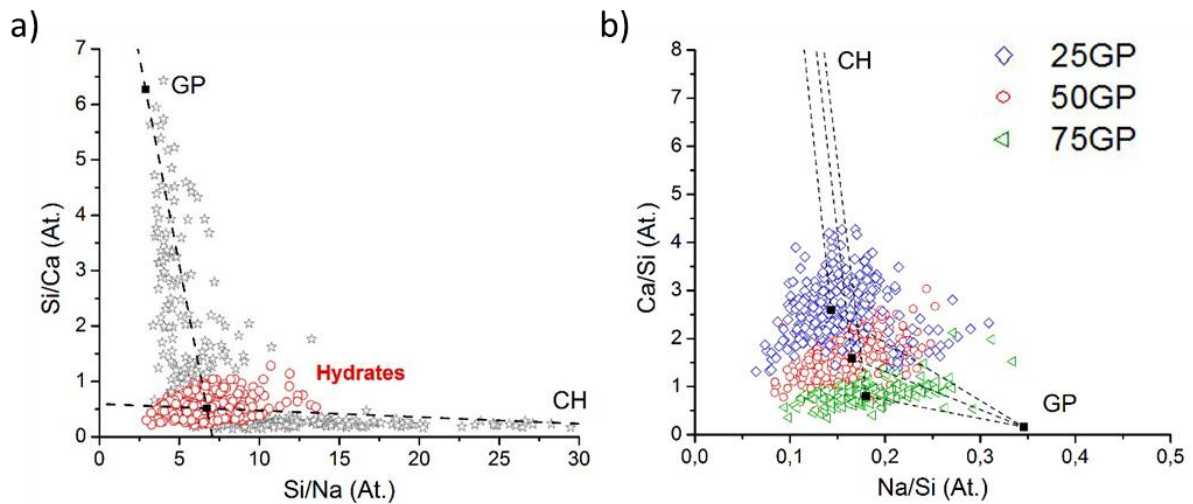
f : Mass fraction of SCM = $(1 - w_{bound\ water,TGA}) \cdot \text{initial ratio in dry blend}$

$w_{bound\ water,TGA}$: Bound water calculated using TGA

321

322 Therefore, in the opposite of cement blends where the stoichiometry of SCM reaction is
 323 usually assumed due to the complexity of the system [8], the composition of the hydrates in
 324 synthetic mixes of GP and CH can be determined correctly. In this aim, two independent
 325 methods were employed at the ages of 28, 56, and 91 days of hydration.

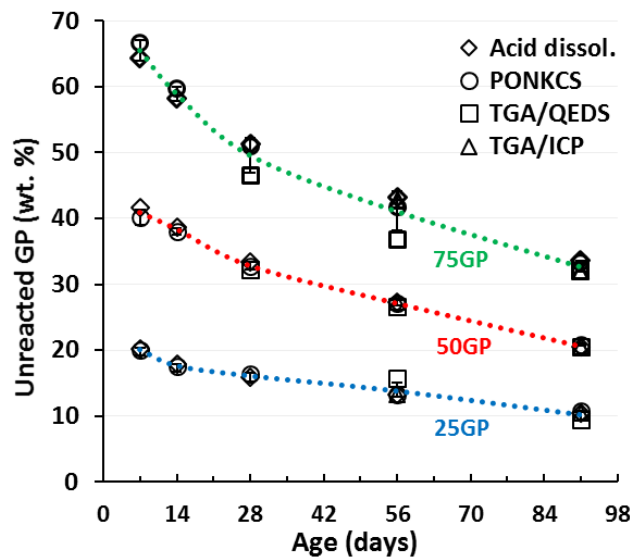
326 First, the composition of the hydrates was determined with EDS by investigating the
 327 chemistry of approximately 700 points per sample. Statistical analyses (multivariate Gaussian
 328 mixture modelling) were then carried, according to the method proposed by Wilson et al.[41–
 329 43], to isolate a cluster of hydration products and determine its mean composition (Si/Ca ;
 330 Si/Na ; $Si/(Ca+Na)$; SOX) and covariance matrix, as shown in Fig 6.



331

332 **Fig. 6. Results of the statistical clustering: a) an example result of the deconvolution method adopted to**
333 **separate the cluster associated to the hydrates, b) the hydrate clusters for the three systems CH-GP after**
334 **91 days of hydration.**

335 Secondly, the filtrates after the acid dissolution were diluted to reach 1 L then analysed using
336 ICP to measure the amounts of Si and Ca. Knowing that the GP remains undissolved after the
337 acid attack, the elements in the solution are mainly provided by the dissolution of the reaction
338 products and the unreacted calcium hydroxide. Therefore, using the results of the TGA to take
339 into account the amount of unreacted CH, the average composition of the product can be
340 determined. These techniques will be, respectively, referred to as TGA/QEDS and TGA/ICP.
341 **Fig. 7** displays the evolution of unreacted GP content in each system as a function of time
342 obtained by the studied techniques.

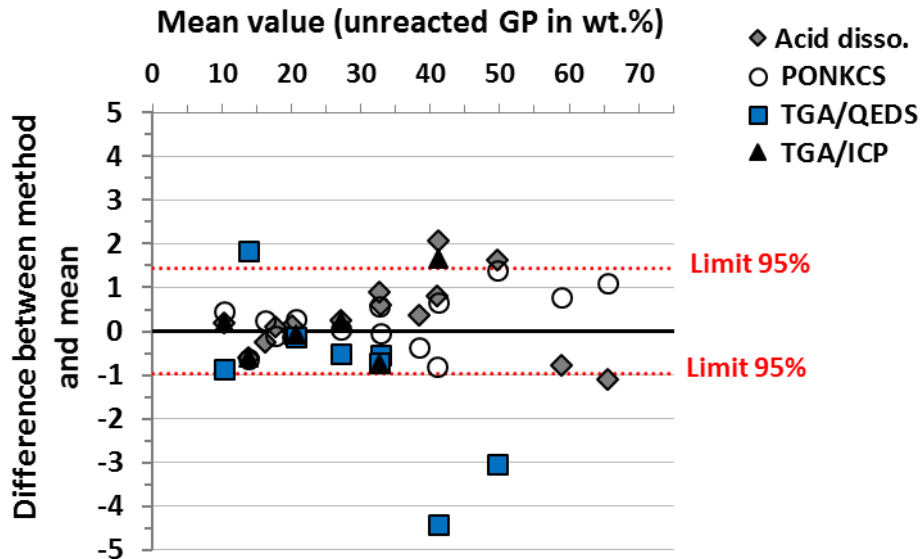


343
344 **Fig. 7. Comparison of the unreacted amount of GP determined by acid dissolution, Rietveld-PONKCS**
345 **and indirectly using TGA/QEDS and TGA/ICP. Dotted lines and error bars show the mean value and the**
346 **standard deviation of the four methods.**

347 **c) Precision and accuracy of the PONKCS method**

348 The accuracy of PONKCS method was assessed by comparing its results to the global mean
349 of the four methods (since the real amount of unreacted GP is not known), while the precision
350 was evaluated by calculating the standard deviation (2σ or 95% confidence interval). As
351 shown in **Fig. 8**, a level of precision (2σ) of 1.2 wt.% and a measurement accuracy of 0.5
352 wt.% in average (max 1.4 wt.%) were found for the unreacted amount of GP in the hydrated
353 GP-CH systems. It was also observed that the accuracy of the PONKCS method tends to
354 decrease when the mixes contain high amounts of GP. Overall, the Rietveld-PONKCS
355 method provided the most consistent results among the studied methods while the
356 TGA/QEDS showed the largest disparities. This might be related to accumulation of errors,

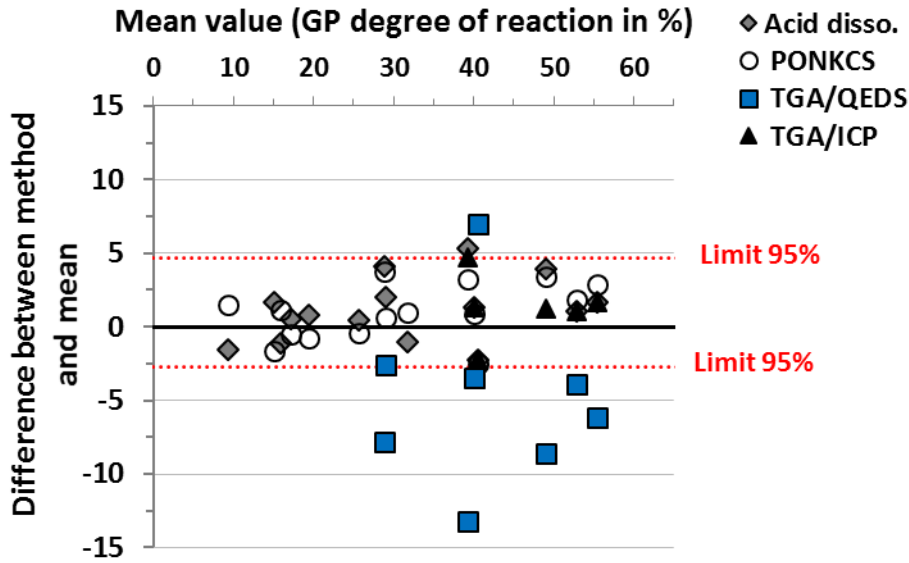
357 since relatively small errors in the determination of the reacted CH content (TGA) can lead to
 358 significant changes in the unreacted amount of GP. Furthermore, the accurate determination
 359 of the composition of hydration products (i.e., the average Ca/Si ratio) can be a difficult task
 360 due to the variability and heterogeneity of the systems.



361
 362 **Fig. 8. Scatter plot of the difference between the measured unreacted amounts of GP and the mean value**
 363 **of the methods, as function of the mean value. Dotted red lines represent the 95% confidence interval for**
 364 **the unreacted amount of GP determined using the PONKCS method.**

365 ***d) Sensitivity analysis and propagation of uncertainties***

366 The PONKCS and acid dissolution methods allow direct quantification of the unreacted GP
 367 content, whereas the other two approaches involve a combination of methods. Thus, even
 368 small experimental errors (e.g. on the Ca/Si ratio of the C-S-H and/or the unreacted GP
 369 content) could lead to higher discrepancies on the degree of hydration, especially when the
 370 initial GP content is low. As shown in Fig. 9, direct methods for the measurement of the
 371 degree of reaction of GP (e.g. acid dissolution, Rietveld-PONKCS) provided the most
 372 consistent results while the indirect method showed relatively larger uncertainties. For the
 373 Rietveld-PONKCS method, an average precision of 3.8% and an accuracy of 1.7% (max
 374 3.4%) were found for the measurement of the degree of reaction. On the other hand, the error
 375 of TGA/QEDS on the measurement of the degree of reaction of GP was assessed to 6.6%
 376 (max 13.3%). In this case, the combined small errors on TGA and/or QEDS measurements
 377 have higher impact on the degree of reaction of SCMs.



378

379 **Fig. 9. Scatter plot of the difference between the GP degree of reaction and the mean value of the methods**
 380 **as function of the mean value. Dotted red lines represent the 95% confidence interval for degree of**
 381 **reaction of GP determined using the PONKCS method.**

382

383 Following the determination of the degree of reaction of GP using Rietveld-PONKCS and
 384 acid dissolution, **equation. 4** was used to back calculate the Ca/Si ratio of the C-S-H using the
 385 reacted amount of portlandite (TGA). Afterwards, the Ca/Si ratio of the products, obtained by
 386 these indirect methods, is compared to the results of direct measurements (QEDS and ICP).
 387 The results, shown in **fig. 10**, highlight the sensitivity of the degree of reaction to even small
 388 variations in the measured Ca/Si ratio. An average error of 0.21 on the Ca/Si ratio of products
 389 was assessed for the Rietveld-PONKCS approach. Also, it should be noted that the
 390 characterisation of the silica-rich rims, which appears around hydrating GP particles [35,40],
 391 is a limiting parameter for the accurate measurement of the Ca/Si ratio of the products using
 392 the EDS point analysis. This might explain the differences with the other techniques.

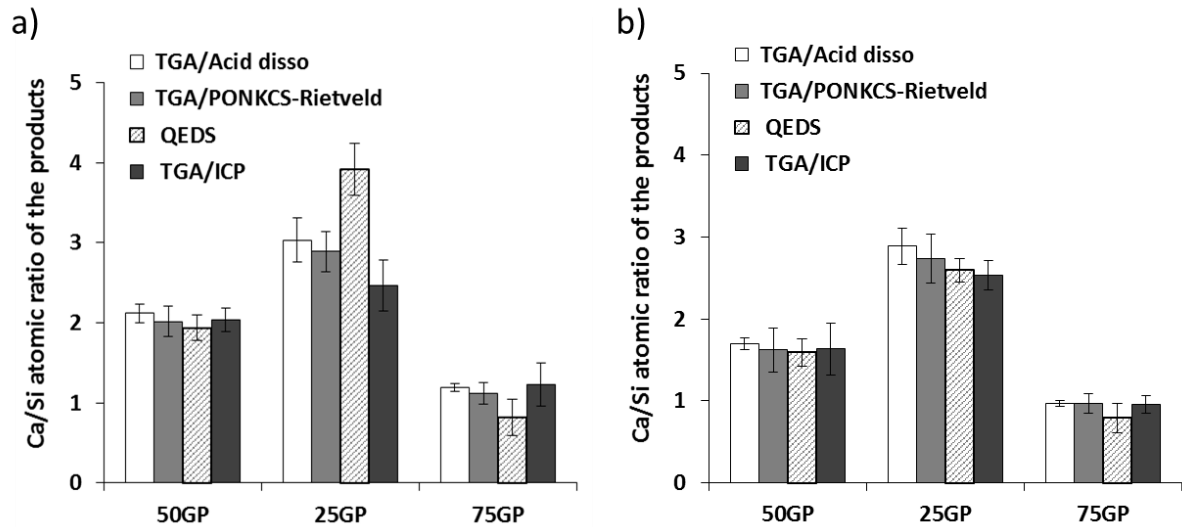


Fig. 10. Comparison of the Ca/Si ratios obtained by the different methods at (a) 56 and (b) 91 days of hydration for the studied systems.

393

394
395

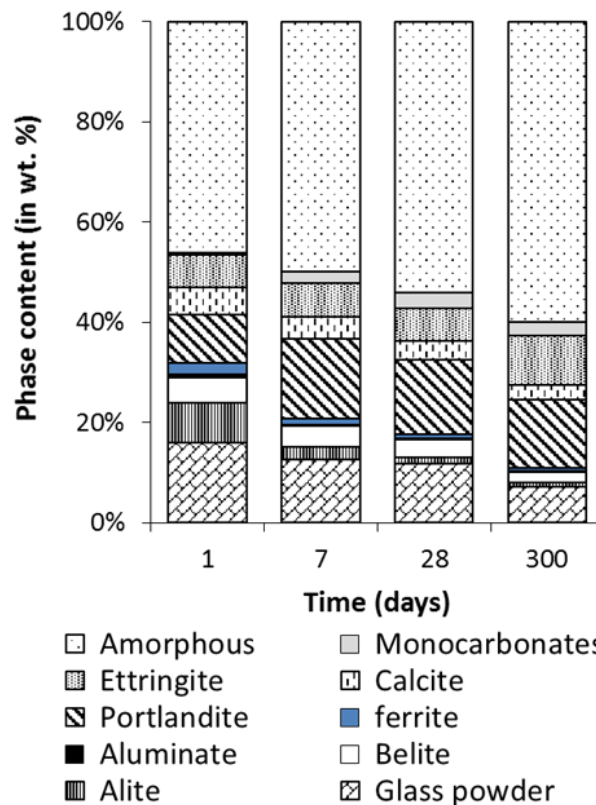
396

397

398 3.3 Application to OPC-GP systems

399 3.3.1 Hydrated blended-cement paste with 20% GP replacement

400 The combination of the Rietveld-PONKCS and the external standard method can provide a
 401 wealth of information concerning the hydrates assemblage in blended cement pastes. In fact,
 402 the changes in the phase composition of the blended cementitious matrix, due to the reactivity
 403 of amorphous SCMs, can be retrieved, both qualitatively and quantitatively ($\pm 1-3$ wt.%). Fig.
 404 11 illustrates the time resolved evolution of the hydrate phase assemblage formed in the
 405 system 20GP (in wt.%). It should be noted that the term “amorphous” in Fig. 11 refers to
 406 poorly crystalline hydrates (e.g. C-S-H, Fe-containing siliceous hydrogarnet, AFm,
 407 hydrotalcite-like phase), which cannot be discerned individually on the XRD patterns.
 408 Overall, the results show a slow hydration kinetics of GP, with ≈ 50 wt.% residual unreacted
 409 GP at 300 days (only $\approx 5\%$ has reacted after 1 day). On the other hand, more than 90% of the
 410 cement clinker has reacted to form C-S-H, portlandite and ettringite, as the main hydration
 411 products. The plausibility of the quantified GP reactivity is assessed subsequently using the
 412 standard addition method.



413

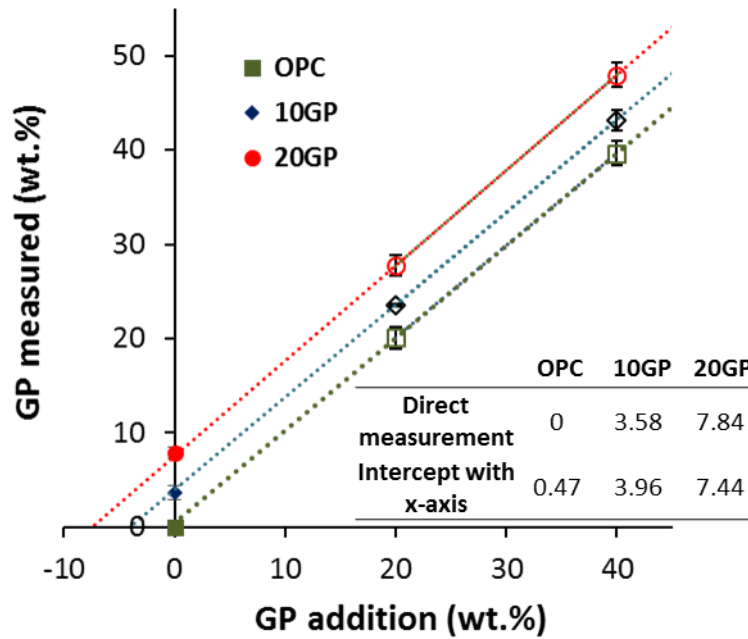
414 **Fig. 11. Evolution of the phase assemblage in hydrating blended cement paste consisting**
 415 **of 80% OPC and 20% GP as a function of time. The amount of reacted GP is quantified**
 416 **using the PONKCS methods while the amorphous phase (which includes C-S-H, Fe-**
 417 **containing siliceous hydrogarnet, AFm, hydrotalcite-like phase) was determined using**
 418 **the external standard method.**

419

420 3.3.2 Accuracy of the quantification of GP in cement pastes

421 For the hydrated blended cement, the accuracy of the method of PONKCS was assessed with
 422 the standard-addition method, i.e., by measuring the total GP content in mixtures of 182-day
 423 hydrated systems (OPC, 10GP and 20GP) with additional 20 and 40 wt.% glass powder. The
 424 positive value for the extrapolate intercept with the x-axis of the systems with additions thus
 425 provides an estimation of the GP in the original sample [6]. As shown in Fig. 12, the
 426 intercepts compare very well with the GP content directly measured by Rietveld-PONKCS,
 427 with a difference of 0.4 wt% on average and 0.5 wt.% at maximum. These differences are
 428 much smaller than the precision range (i.e. 95% confidence interval) of the method that was
 429 assessed to 1.6 wt.% on average (max 3.4 wt.%), using independent replicates.

430



431

432 **Fig. 12.** Measured amount of GP using Rietveld-PONKCS method as a function of the additional GP
 433 mixed with ground samples of 182 days hydrated blended systems (OPC, 10GP and 20GP). The error bars
 434 show the repeatability of the measurement while the positive value for the intercept with the x-axis gives
 435 an estimation of the GP content in the original samples.

436

437 4. Discussion

438 This paper presents an assessment of the accuracy and precision of the Rietveld-PONKCS
 439 method for the quantification of amorphous phases in anhydrous and hydrated systems. The
 440 proposed approach allowed a direct determination of the contribution of amorphous SCMs
 441 and C-S-H (by difference using a standard) in hydrating binders. The glass powder content in
 442 blended and hydrated systems of increasing complexity was investigated by cross-checking
 443 the results of independent characterisation techniques. For anhydrous binary mixes consisting
 444 of GP-CH/Corundum, the quantification method produced high accuracy, with a weighed-
 445 measured bias fewer than 1.5 wt.%. For hydrating synthetic mixes of CH and GP, the
 446 correctness of the method was assessed by comparison to the global mean of the four studied
 447 approaches. Overall, the results of the Rietveld-PONKCS method compared well to the
 448 results of acid dissolution and TGA/ICP methods. The average differences between the mean
 449 of the methods and the result of each method were respectively 0.5, 0.7 and 0.6 wt.% for
 450 Rietveld-PONKCS, acid dissolution and TGA/ICP. On the other hand, TGA/QEDS analyses
 451 provided the largest variation among the studied approaches, with an average difference with
 452 the mean of 1.5 wt.% (max 4.4 wt.%). However, it should be emphasised, as aforementioned,
 453 that the accuracy was discussed in this study only in terms of comparison to the global mean

454 (the real amount of unreacted GP remains unknown). Finally, in the GP-blended cement
455 pastes, the accuracy was estimated to 0.4 wt.% using the standard-addition method.

456 In the case of GP, a global level of precision lower than 3 wt.% was found for the Rietveld-
457 PONKCS method for both anhydrous and hydrated blends. However, even small errors on the
458 unreacted GP content could lead to larger disparities in the degree of reaction of GP. For
459 instance, in the extreme case of the 10GP system hydrated for 182 days, a measurement error
460 of ± 1 wt.% in the GP content could result in a scatter of $\pm 15\%$ in degree of reaction.
461 Consequently, it should be acknowledged that the accuracy of the Rietveld-PONKCS method
462 for GP can drop acutely at high degrees of reaction or/and low replacement rates (e.g. below
463 10 wt.%) due the estimated precision of 2-3 wt.%. In this case, several replicate testing are
464 needed to improve the statistical certainty and the reliability of the results. Furthermore, it is
465 worth mentioning that even though the Rietveld-PONKCS method showed promising results
466 for glass powder and that no specific hypothesis on the materials composition was necessary
467 for its application, these results might not be reproducible for other SCMs. First, the glass
468 powder has a homogeneous composition, thus it is realistic to assume that the calibrated phase
469 is still representative of GP even after its partial dissolution. Second, the overlap between the
470 GP and C-S-H peaks is minimal, thus the decomposition of the XRD pattern is relatively easy.
471 These conditions do not necessarily apply for materials such as fly ash due its heterogeneity
472 [44] or slag due to the important overlap between its diffuse hump and the C-S-H contribution
473 [7]. Similar observations were reported by previous work on the PONKCS method [6,33].

474 In addition, an improvement of the quantification could be achieved by calibrating the
475 PONKCS phase on pre-blended sample with a similar composition of the unknown sample,
476 instead of a sample containing only the phase of interest. To explore this approach, the
477 pseudo-phase of GP was recalibrated using a sample of 182-day hydrated OPC mixed with 20
478 wt.% GP addition before the application to GP-blended cement pastes. Notably, no significant
479 change was observed on the ZMV value of GP, even if this procedure allowed taking into
480 consideration the presence or the absence of elements absorbing X-rays such as calcium, iron
481 and potassium. Moreover, the incorporation of minor elements (such Al, Na, Mg...) in the C-
482 S-H structure may lead to a change in the C-S-H XRD profile. Therefore, additional
483 improvements of the fit could also be reached with a more adapted C-S-H peak phase profile
484 for hydrated blended cements [6,45].

485 Overall, it can be concluded that the Rietveld-PONKCS method enables a direct
486 quantification of amorphous phase with a similar accuracy to other techniques such as

487 selective acid dissolution and TGA/ICP. Furthermore, the Rietveld-PONKCS has notable
488 advantages compared to other techniques. First, the method after calibration requires only X-
489 ray diffraction pattern to quantify both the crystalline and amorphous phases in the sample.
490 Second, the direct quantification of GP avoids the accumulation of errors, which is
491 encountered in indirect methods. Third, the method can also be applied to other SCMs,
492 provided a homogeneous composition and no overlap of its amorphous hump with that of the
493 C-S-H. Finally, additional work is still required to attain a more widespread use of the
494 method, with investigations of the interlaboratory consistency and reproducibility. Eventually,
495 further work will aim at developing and testing an optimised analysis protocol with guidelines
496 and specifications concerning: the definition of the background, the number of refined
497 parameters and their variation range, the definition and the calibration of the pseudo-phase,
498 the size of particles, the limitations of the method, and more.

499

500 **5. Conclusion**

501 In this work, the Rietveld-PONKCS method was applied for the quantification of the degree
502 of reaction of glass powder in anhydrous and hydrated binary pastes of CH-GP and OPC-GP.
503 The following conclusions can be drawn according to the main findings of this study:

- 504 1. The precision (repeatability) of the measurement of GP content by the Rietveld-
505 PONKCS method was assessed to 1.6 wt.% on average while the accuracy (bias) of
506 the method was lower than 1.5 wt.%.
- 507 2. The Rietveld-PONKCS method showed a similar accuracy to acid dissolution and
508 TGA/ICP. On the other hand, the indirect method based on TGA/QEDS produced the
509 largest disparities. This is likely related to the complexity of the determination of
510 Ca/Si and to the sensitivity of the approach to errors in the Ca/Si ratio and portlandite
511 consumption.
- 512 3. The main advantages of the Rietveld-PONKCS method are the ease and speed of the
513 analyses, the fact that it is a direct measurement and that no assumptions are required
514 (errors are not accumulated), and the comprehensive information which can be
515 retrieved from a single experimental test (XRD analysis).
- 516 4. Despite the apparent simplicity of the PONKCS method, the analyst experience and a
517 good knowledge in crystallography are prerequisite to reach a good analytical
518 accuracy and meaningful results. In addition, further effort and crosschecking work

519 are necessary for the development of an optimised and standardised analysis
520 procedure.

521 Given the promising results of the Rietveld-PONKCS approach, this method is expected to
522 quickly become a standard tool in the material science of cement and concrete, with its
523 particular use to evaluate the reactivity of amorphous SCMs. Moreover, the choice of high
524 quality SCMs can be facilitated through the assessment of their influence on the hydrates
525 phase assemblage and, with further development, the prediction of their impact on the long
526 term properties of concrete.

527

528 **5. Acknowledgements**

529 This study was carried out in the frame of the International Associated Laboratory LIA-
530 EcoMat and funded by IFSTTAR (France) and the University of Sherbrooke (Canada). The
531 authors gratefully acknowledge the financial support of the SAQ Industrial Chair on
532 Valorization of Glass in Materials.

533

534 **References**

535

- 536 [1] B. Lothenbach, K. Scrivener, R.D.D. Hooton, Supplementary cementitious materials,
537 *Cem. Concr. Res.* 41 (2011) 1244–1256. doi:10.1016/j.cemconres.2010.12.001.
- 538 [2] H.F.W. Taylor, *Cement chemistry*. 2nd ed., Acad. Press. 20 (1997) 335.
539 doi:10.1016/S0958-9465(98)00023-7.
- 540 [3] M.C.G. Juenger, R. Siddique, Recent advances in understanding the role of
541 supplementary cementitious materials in concrete, *Cem. Concr. Res.* 78 (2015) 71–80.
542 doi:10.1016/J.CEMCONRES.2015.03.018.
- 543 [4] M. Thomas, *Supplementary cementing materials in concrete*, CRC press, 2013.
- 544 [5] N. Schwarz, H. Cam, N. Neithalath, Influence of a fine glass powder on the durability
545 characteristics of concrete and its comparison to fly ash, *Cem. Concr. Compos.* 30
546 (2008) 486–496. doi:10.1016/j.cemconcomp.2008.02.001.
- 547 [6] R. Snellings, A. Salze, K.L. Scrivener, Use of X-ray diffraction to quantify amorphous
548 supplementary cementitious materials in anhydrous and hydrated blended cements,
549 *Cem. Concr. Res.* 64 (2014) 89–98. doi:10.1016/J.CEMCONRES.2014.06.011.
- 550 [7] P.T. Durdziński, M. Ben Haha, S.A. Bernal, N. De Belie, E. Gruyaert, B. Lothenbach,
551 E. Menéndez Méndez, J.L. Provis, A. Schöler, C. Stabler, Z. Tan, Y. Villagrán
552 Zaccardi, A. Vollpracht, F. Winnefeld, M. Zajac, K.L. Scrivener, Outcomes of the
553 RILEM round robin on degree of reaction of slag and fly ash in blended cements,
554 *Mater. Struct. Constr.* 50 (2017) 135. doi:10.1617/s11527-017-1002-1.

- 555 [8] K.L. Scrivener, B. Lothenbach, N. De Belie, E. Gruyaert, J. Skibsted, R. Snellings, A.
556 Vollpracht, TC 238-SCM: hydration and microstructure of concrete with SCMs, Mater.
557 Struct. 48 (2015) 835–862. doi:10.1617/s11527-015-0527-4.
- 558 [9] K. Scrivener, R. Snellings, B. Lothenbach, A Practical Guide to Microstructural
559 Analysis of Cementitious Materials, 2016. doi:10.7693/wl20150205.
- 560 [10] S. Li, D.M. Roy, A. Kumar, Quantitative determination of pozzolanas in hydrated
561 systems of cement or Ca(OH)₂ with fly ash or silica fume, Cem. Concr. Res. 15 (1985)
562 1079–1086. doi:10.1016/0008-8846(85)90100-0.
- 563 [11] H. Maraghechi, M. Maraghechi, F. Rajabipour, C.G. Pantano, Pozzolanic reactivity of
564 recycled glass powder at elevated temperatures: Reaction stoichiometry, reaction
565 products and effect of alkali activation, Cem. Concr. Compos. 53 (2014) 105–114.
566 doi:10.1016/J.CEMCONCOMP.2014.06.015.
- 567 [12] K. Luke, F.P. Glasser, Selective dissolution of hydrated blast furnace slag cements,
568 Cem. Concr. Res. 17 (1987) 273–282. doi:10.1016/0008-8846(87)90110-4.
- 569 [13] V. Kocaba, Development and evaluation of methods to follow microstructural
570 development of cementitious systems including slags, EPFL, 2009. doi:10.5075/epfl-
571 thesis-4523.
- 572 [14] M. Ben Haha, K. De Weerd, B. Lothenbach, Quantification of the degree of reaction
573 of fly ash, Cem. Concr. Res. 40 (2010) 1620–1629.
574 doi:10.1016/j.cemconres.2010.07.004.
- 575 [15] S. Ohsawa, K. Asaga, S. Goto, M. Daimon, Quantitative determination of fly ash in the
576 hydrated fly ash - CaSO₄·2H₂O□Ca(OH)₂ system, Cem. Concr. Res. 15 (1985) 357–
577 366. doi:10.1016/0008-8846(85)90047-X.
- 578 [16] V. Kocaba, E. Gallucci, K.L. Scrivener, Methods for determination of degree of
579 reaction of slag in blended cement pastes, Cem. Concr. Res. 42 (2012) 511–525.
580 doi:10.1016/J.CEMCONRES.2011.11.010.
- 581 [17] F. Avet, X. Li, K. Scrivener, Determination of the amount of reacted metakaolin in
582 calcined clay blends, Cem. Concr. Res. 106 (2018) 40–48.
583 doi:10.1016/J.CEMCONRES.2018.01.009.
- 584 [18] E.M.J. Berodier, Impact of the Supplementary Cementitious Materials on the kinetics
585 and microstructural development of cement hydration, 6417 (2015) 1–136.
- 586 [19] K.L. Scrivener, B. Lothenbach, N. De Belie, E. Gruyaert, J. Skibsted, R. Snellings, A.
587 Vollpracht, TC 238-SCM: hydration and microstructure of concrete with SCMs: State
588 of the art on methods to determine degree of reaction of SCMs, Mater. Struct. Constr.
589 48 (2015) 835–862. doi:10.1617/s11527-015-0527-4.
- 590 [20] P.-Y. Mahieux, J.-E. Aubert, M. Cyr, M. Coutand, B. Husson, Quantitative
591 mineralogical composition of complex mineral wastes – Contribution of the Rietveld
592 method, Waste Manag. 30 (2010) 378–388. doi:10.1016/J.WASMAN.2009.10.023.
- 593 [21] P. Stutzman, Powder diffraction analysis of hydraulic cements: ASTM Rietveld round-
594 robin results on precision, Powder Diffr. 20 (2005) 97–100. doi:10.1154/1.1913712.
- 595 [22] M. García-Maté, G. Álvarez-Pinazo, L. León-Reina, A.G. De la Torre, M.A.G. Aranda,
596 Rietveld quantitative phase analyses of SRM 2686a: A standard Portland clinker, Cem.
597 Concr. Res. 115 (2019) 361–366. doi:10.1016/J.CEMCONRES.2018.09.011.
- 598 [23] P.E. Stutzman, Direct Determination of Phases in Portland Cements by Quantitative X-

- 599 Ray Powder Diffraction | NIST, Tech. Note (NIST TN) -. (2010).
600 [https://www.nist.gov/publications/direct-determination-phases-portland-cements-](https://www.nist.gov/publications/direct-determination-phases-portland-cements-quantitative-x-ray-powder-diffraction)
601 [quantitative-x-ray-powder-diffraction](https://www.nist.gov/publications/direct-determination-phases-portland-cements-quantitative-x-ray-powder-diffraction) (accessed June 4, 2019).
- 602 [24] M.A.G. Aranda*, A.G. De la Torre, L. Leon-Reina, Rietveld Quantitative Phase
603 Analysis of OPC Clinkers, Cements and Hydration Products, *Rev. Mineral.*
604 *Geochemistry.* 74 (2012) 169–209. doi:10.2138/rmg.2012.74.5.
- 605 [25] G. Le Saoût, V. Kocaba, K. Scrivener, Application of the Rietveld method to the
606 analysis of anhydrous cement, *Cem. Concr. Res.* 41 (2011) 133–148.
607 doi:10.1016/J.CEMCONRES.2010.10.003.
- 608 [26] H.M. Rietveld, IUCr, A profile refinement method for nuclear and magnetic structures,
609 *J. Appl. Crystallogr.* 2 (1969) 65–71. doi:10.1107/S0021889869006558.
- 610 [27] A.G. De, L. Torre, S. Bruque, M.A.G. Aranda, Rietveld quantitative amorphous
611 content analysis, *J. Appl. Cryst.* 34 (2001) 196–202.
612 <https://journals.iucr.org/j/issues/2001/02/00/ks0064/ks0064.pdf> (accessed April 14,
613 2018).
- 614 [28] P.M. Suherman, A. van Riessen, B. O’Connor, D. Li, D. Bolton, H. Fairhurst,
615 Determination of amorphous phase levels in Portland cement clinker, *Powder Diffr.* 17
616 (2002) 178–185. doi:10.1154/1.1471518.
- 617 [29] D. Jansen, C. Stabler, F. Goetz-Neunhoeffler, S. Dittrich, J. Neubauer, Does Ordinary
618 Portland Cement contain amorphous phase? A quantitative study using an external
619 standard method, *Powder Diffr.* 26 (2011) 31–38. doi:10.1154/1.3549186.
- 620 [30] N.V.Y. Scarlett, I.C. Madsen, Quantification of phases with partial or no known crystal
621 structures, *Powder Diffr.* 21 (2006) 278–284. doi:10.1154/1.2362855.
- 622 [31] Z. Sun, A. Vollpracht, Isothermal calorimetry and in-situ XRD study of the NaOH
623 activated fly ash, metakaolin and slag, *Cem. Concr. Res.* 103 (2018) 110–122.
624 doi:10.1016/J.CEMCONRES.2017.10.004.
- 625 [32] Y.P. Stetsko, N. Shanahan, H. Deford, A. Zayed, Quantification of supplementary
626 cementitious content in blended Portland cement using an iterative Rietveld-PONKCS
627 technique, *J. Appl. Crystallogr.* 50 (2017) 498–507. doi:10.1107/S1600576717002965.
- 628 [33] C. Naber, S. Stegmeyer, D. Jansen, F. Goetz-Neunhoeffler, J. Neubauer, The PONKCS
629 method applied for time resolved XRD quantification of supplementary cementitious
630 material reactivity in hydrating mixtures with ordinary Portland cement, *Constr. Build.*
631 *Mater.* 214 (2019) 449–457. doi:10.1016/J.CONBUILDMAT.2019.04.157.
- 632 [34] G.V.P. Bhagath Singh, K.V.L. Subramaniam, Quantitative XRD Analysis of Binary
633 Blends of Siliceous Fly Ash and Hydrated Cement, *J. Mater. Civ. Eng.* 28 (2016)
634 04016042. doi:10.1061/(ASCE)MT.1943-5533.0001554.
- 635 [35] R. Idir, M. Cyr, A. Tagnit-Hamou, Pozzolanic properties of fine and coarse color-
636 mixed glass cullet, *Cem. Concr. Compos.* 33 (2011) 19–29.
637 doi:10.1016/j.cemconcomp.2010.09.013.
- 638 [36] K. Zheng, Pozzolanic reaction of glass powder and its role in controlling alkali-silica
639 reaction, *Cem. Concr. Compos.* 67 (2016). doi:10.1016/j.cemconcomp.2015.12.008.
- 640 [37] D.C. Creagh, J.H. Hubbell, X-ray absorption (or attenuation) coefficients, in: E. Prince
641 (Ed.), *Int. Tables Crystallography, Vol.C Math. Phys. Chem. Tables* (3th Ed., 2004: pp.
642 230–236.

- 643 [38] I.C. Madsen, N.V.Y. Scarlett, A.A. Kern, Description and survey of methodologies for
644 the determination of amorphous content via X-ray powder diffraction, *Zeitschrift Fur*
645 *Krist.* 226 (2011) 944–955. doi:10.1524/zkri.2011.1437.
- 646 [39] E. Bonaccorsi, S. Merlino, A.R. Kampf, The Crystal Structure of Tobermorite 14 A
647 (Plombierite), a C-S-H Phase, *J. Am. Ceram. Soc.* 88 (2005) 505–512.
648 doi:10.1111/j.1551-2916.2005.00116.x.
- 649 [40] M. Mejdı, W. Wilson, M. Saillio, T. Chaussadent, L. Divet, A. Tagnit-Hamou,
650 Investigating the pozzolanic reaction of post-consumption glass powder and the role of
651 portlandite in the formation of sodium-rich C-S-H, *Cem. Concr. Res.* 123 (2019)
652 105790. doi:10.1016/j.cemconres.2019.105790.
- 653 [41] W. Wilson, L. Sorelli, A. Tagnit-Hamou, Automated coupling of NanoIndentation and
654 Quantitative Energy-Dispersive Spectroscopy (NI-QEDS): A comprehensive method to
655 disclose the micro-chemo-mechanical properties of cement pastes, *Cem. Concr. Res.*
656 103 (2018) 49–65. doi:10.1016/J.CEMCONRES.2017.08.016.
- 657 [42] W. Wilson, L. Sorelli, A. Tagnit-Hamou, Unveiling micro-chemo-mechanical
658 properties of C-(A)-S-H and other phases in blended-cement pastes, *Cem. Concr. Res.*
659 107 (2018) 317–336. doi:10.1016/J.CEMCONRES.2018.02.010.
- 660 [43] K. J. Krakowiak, W. Wilson, S. James, S. Musso, F.-J. Ulm, Inference of the phase-to-
661 mechanical property link via coupled X-ray spectrometry and indentation analysis:
662 Application to cement-based materials, *Cem. Concr. Res.* 67 (2015) 271–285.
663 doi:10.1016/J.CEMCONRES.2014.09.001.
- 664 [44] P.T. Durdziński, C.F. Dunant, M. Ben Haha, K.L. Scrivener, A new quantification
665 method based on SEM-EDS to assess fly ash composition and study the reaction of its
666 individual components in hydrating cement paste, *Cem. Concr. Res.* 73 (2015) 111–
667 122. doi:10.1016/j.cemconres.2015.02.008.
- 668 [45] S.T. Bergold, F. Goetz-Neunhoeffler, J. Neubauer, Quantitative analysis of C-S-H in
669 hydrating alite pastes by in-situ XRD, *Cem. Concr. Res.* 53 (2013) 119–126.
670 doi:10.1016/j.cemconres.2013.06.001.
- 671